

## Development of High-Surface-Area Alumina-Supported Catalysts for the Generation of Hydrogen from NaBH<sub>4</sub>

\*Makale Bilgisi / Article Info

Alındı/Received: 13.07.2024

Kabul/Accepted: 02.09.2024

Yayımlandı/Published: xx.xx.xxxx

### NaBH<sub>4</sub>'ten Hidrojen Üretimi için Yüksek Yüzey Alanlı Alümina Destekli Katalizörlerin Geliştirilmesi

Meltem KARAIŞMAİLOĞLU ELİBOL\* 

Turkish-German University, Faculty of Natural Sciences, Department of Energy Science and Technology, Istanbul, Türkiye

© Afyon Kocatepe Üniversitesi

© 2025 The Author | Creative Commons Attribution-Noncommercial 4.0 (CC BY-NC) International License



#### Abstract

Hydrogen as a valuable energy carrier plays a significant role in renewable energy technologies to reduce the greenhouse gas emission into the atmosphere. However, natural hydrogen gas does not exist in the universe and should be gained from hydrogen-containing compounds. In this regard, metal hydrides are excellent candidates for producing hydrogen gas. Among complex metal hydrides, sodium borohydride (NaBH<sub>4</sub>) possesses its advantages due to its enhanced hydrogen storage capacity and low cost. In the present study, hydrogen gas was generated through the catalytic hydrolysis of NaBH<sub>4</sub>. In this regard, high-surface-area alumina-supported Ni/Al<sub>2</sub>O<sub>3</sub>, NiCo/Al<sub>2</sub>O<sub>3</sub>, and Ru-NiCo/Al<sub>2</sub>O<sub>3</sub> catalysts have been prepared via wash coating method and tested in a continuous flow reactor. The results indicate that the Ru-NiCo/Al<sub>2</sub>O<sub>3</sub> catalyst with a specific surface area of 154.40 m<sup>2</sup>·g<sup>-1</sup> showed the highest initial catalytic activity of 0.031 mmol·s<sup>-1</sup>·g<sup>-1</sup> but with a rapid loss in its activity. Compared to that, despite a lower initial catalytic activity in the presence of the NiCo/Al<sub>2</sub>O<sub>3</sub> catalyst, the hydrogen generation kept rising during the reaction, and 225 mL H<sub>2</sub> was produced after 100 min. Therefore, the NiCo/Al<sub>2</sub>O<sub>3</sub> catalyst with a surface area of 165.84 m<sup>2</sup>·g<sup>-1</sup> can be proposed as a promising alternative.

**Keywords:** Sodium borohydride; Hydrolysis; Hydrogen; Alumina; Catalyst

#### Öz

Değerli bir enerji taşıyıcısı olan hidrojen, yenilenebilir enerji teknolojilerinde atmosfere sera gazı emisyonunun azaltılmasında önemli bir rol oynamaktadır. Ancak hidrojen gazı doğada mevcut olmayıp hidrojen içeren bileşiklerden elde edilmesi gerekmektedir. Metal hidrürler hidrojen gazı üretimi için mükemmel adaylardır. Karmaşık metal hidrürler arasında sodyum borhidür (NaBH<sub>4</sub>), gelişmiş hidrojen depolama kapasitesi ve düşük maliyeti gibi çeşitli avantajlara sahiptir. Bu çalışmada katalitik hidroliz yoluyla NaBH<sub>4</sub>'ten hidrojen gazı üretilmektedir. Bu amaçla yıkayarak kaplama yöntemi ile yüksek yüzey alanına sahip alümina destekli Ni/Al<sub>2</sub>O<sub>3</sub>, NiCo/Al<sub>2</sub>O<sub>3</sub> ve Ru-NiCo/Al<sub>2</sub>O<sub>3</sub> yapıları katalizörler hazırlanmış olup bu katalizörler sürekli akışlı reaktörde test edilmiştir. Elde edilen sonuçlara göre yüzey alanı 154.40 m<sup>2</sup>·g<sup>-1</sup> olan Ru-NiCo/Al<sub>2</sub>O<sub>3</sub> yapıları katalizör başlangıçta 0.031 mmol·s<sup>-1</sup>·g<sup>-1</sup> değerinde en yüksek katalitik aktiviteye sahip olup reaksiyon boyunca aktivitesinde hızlı bir azalma gözlemlenmiştir. NiCo/Al<sub>2</sub>O<sub>3</sub> yapıları katalizörün varlığında ise başlangıçta daha düşük bir katalitik aktivite görülmesine rağmen reaksiyon boyunca hidrojen üretimi hızla artmaya devam etmiş olup 100 dk. sonra 225 ml H<sub>2</sub> gazı üretilmiştir. Bu nedenle 165.84 m<sup>2</sup>·g<sup>-1</sup> yüzey alanına sahip NiCo/Al<sub>2</sub>O<sub>3</sub> yapıları katalizör alternatif olarak önerilebilir.

**Anahtar Kelimeler:** Sodyum borhidür; Hidroliz; Hidrojen; Alümina; Katalizör

#### 1. Introduction

Air pollution with the following issue “climate change” is one of the most important issues for societies. Using fossil fuels as energy sources harms air quality. Through the combustion of fossil fuels, the amount of atmospheric carbon dioxide (CO<sub>2</sub>) is increased. The increase in the CO<sub>2</sub> amount causes the formation of CO<sub>2</sub> layer around the earth resulting in global warming (Baykara et al. 2022). Hence, the utilization of alternative energy sources is essential to reduce CO<sub>2</sub> emissions. In this respect, hydrogen is a valuable energy carrier, and its reaction with the air produces just water. On the one hand, the usage of hydrogen as an energy carrier can mostly cover the energy demand, on the other hand, it reduces CO<sub>2</sub>

emissions because of its carbon-free nature (Baykara et al. 2018). Compared to the storage of fossil fuels, the storage of hydrogen gas is challenging and still needs to be improved (Zhu et al. 2023). In this regard, metal hydrides are good candidates to store hydrogen, conveniently. They are classified as binary, intermetallic, and complex hydrides. This type of material has the potential to desorb the pre-absorbed hydrogen atoms forming the hydrogen gas. Binary metal hydrides in a nominal chemical formula of MH<sub>x</sub> consist of a main group or transition metal and hydrogen (Luo et al. 2020). AB<sub>x</sub>Y<sub>x</sub> represents intermetallic metal hydrides, herein, A and B are for hydrating and non-hydrating metals, respectively (Schneemann et al. 2018). Complex hydrides shown as MEM<sub>x</sub> include alkaline metal cations and hydrogen-

containing anions such as alanates (AlH<sub>4</sub><sup>-</sup>) and borohydrides (BH<sub>4</sub><sup>-</sup>) and possess the highest hydrogen storage capacity (Schneemann et al. 2018). Hydrolysis of complex metal hydrides is a convenient method to release hydrogen at ambient temperature. LiBH<sub>4</sub>, NaBH<sub>4</sub> and Mg(BH<sub>4</sub>)<sub>2</sub> possess high hydrogen storage capacity and are suitable for obtaining hydrogen via the hydrolysis process (Zhu et al. 2023, Laversenne et al. 2008)). In the presence of these metal hydrides, hydrogen obtained has a high purity required for real-time proton membrane fuel cell applications. LiBH<sub>4</sub> possesses the highest hydrogen storage capacity with 13.9 wt%, however, due to its enhanced cost, it is hard to use for large-scale applications. Mg(BH<sub>4</sub>)<sub>2</sub> with its hydrogen capacity of 12.8 wt% is another candidate for hydrolysis processes, but a large amount of heat is released during the reaction. In addition, toxic B<sub>2</sub>H<sub>6</sub> is produced as a byproduct that makes the process unfavorable (Solovev et al. 2018).

Regarding its lower price and non-toxic byproduct during hydrolysis, NaBH<sub>4</sub> gained more attraction to release hydrogen at ambient temperature. Several studies have been conducted to enhance the hydrogen evolution rate through catalytic hydrolysis (Balkanli and Figen 2019, Özkar and Zahmakiran 2005, Xu et al. 2024, Zhu et al. 2023). In the presence of noble metals, high catalytic activity has been reported (Patel and Miotello 2015), however, the higher cost of noble metals is a significant reason for developing of alternative catalysts with transition metals. Additionally, unsupported catalysts suffer from the agglomeration of its particles which leads to a decrease in catalytic activity. Hence, the utilization of support materials is inevitable (Fernandes et al. 2009). Several studies have been focused on the implementation of noble metals such as Ru, Pt, Pd, and Rh on the carbon nanotubes (CNTs) or cobalt oxide (Co<sub>3</sub>O<sub>4</sub>) supports (Bozkurt et al. 2019, Uzundurukan and Devrim 2019, Zhang et al. 2021). Catalysts which include non-noble metals such as Co, Ni, Fe, and Cu exhibit relatively good performance in hydrolysis of NaBH<sub>4</sub> (Filiz and Figen 2019, Wang et al. 2021). Furthermore, their lower cost compared to the noble-metal-included catalysts widens their application in this process.

Regarding the necessity of support materials in catalyst development for the hydrolysis of NaBH<sub>4</sub>, high-surface-area alumina (Al<sub>2</sub>O<sub>3</sub>) pellets were used in this study. Alumina pellets were coated with Ni-Co alloy and doped with Ru to be tested in hydrolysis of NaBH<sub>4</sub>. The as-prepared catalysts have been characterized by BET, ICP-MS, and XRD analyses, and their catalytic performances were tested in a continuous reactor under the flow of NaBH<sub>4</sub> solution.

## 2. Materials and Methods

### 2.1 Synthesis of catalysts

In this study, three different Al<sub>2</sub>O<sub>3</sub>-supported catalysts were prepared via the wash coating method listed in Table 1. The synthesis procedure consists of three steps. For the preparation of 1M precursor solutions, the appropriate amount of metal salts (NiN<sub>2</sub>O<sub>6</sub>·6H<sub>2</sub>O, Alfa Aesar, Co(NO<sub>3</sub>)<sub>2</sub>·6H<sub>2</sub>O, Carlo Erba and RuCl<sub>3</sub>·xH<sub>2</sub>O), Merck) were dissolved in deionized water, and citric acid was added as chelate agent ( $n_{\text{nitric acid}}:n_{\text{metal cation}}=1.5$ ). The pH of each solution was adjusted to 7 with ammonia solution. In the second step, Al<sub>2</sub>O<sub>3</sub> pellets (Alfa Aesar, high surface catalyst support) were washed in the precursor solutions several times and then oven-dried at 225 °C. In the last step, they have been calcined at 700 °C for 2h. For the synthesis of Ru-NiCo/Al<sub>2</sub>O<sub>3</sub> catalysts, Al<sub>2</sub>O<sub>3</sub> pellets were firstly washed in 1M precursor solution including nickel- and cobalt salts and calcined at 700 °C for 2 h. NiCo/Al<sub>2</sub>O<sub>3</sub> pellets obtained after the first calcination step were washed in 0.05 M precursor solution consisting of Ru salt. After this step, pellets were recalcined at 500 °C for 2h.

### 2.2 Characterization of catalysts

The crystalline phases of all samples were determined by XRD analyses. XRD measurements were conducted by a Philips Panalytical EMPYREAN X-ray diffractometer (XRD) in a diffraction angle range of 10° to 90° with CuK $\alpha$  radiation. Brunauer–Emmett–Teller (BET) isotherm technique was used to determine the specific surface area of all samples. BET measurements were carried out by nitrogen adsorption using Micromeritics Gemini VII BET Instrument. Before BET measurements, each sample was pretreated at 300 °C for 12h to remove the humidity from the sample. The metal contents in each sample were determined by Agilent Technologies 7700x inductively coupled plasma mass spectrometry (ICP-MS). Prior to measurements, samples were prepared for analysis in ETHOS EASY MILESTONE microwave acid digestion system at 210 °C.

### 2.3 Catalytic hydrolysis of NaBH<sub>4</sub>

The catalytic hydrolysis of NaBH<sub>4</sub> was carried out in an integrated continuous system as shown in Figure 1. To prevent self-hydrolysis of NaBH<sub>4</sub> at ambient temperature (Schlesinger et al. 1953), firstly, an 0.5 M alkaline solution of NaBH<sub>4</sub> ( $c_{\text{NaBH}_4}:c_{\text{NaOH}}=1:1$ ) was prepared, and the solution was fed to the reactor (filled with 1.7 g catalyst) by a peristaltic pump with the flow rate of 3 ml·min<sup>-1</sup>. The amount of generated hydrogen gas was determined by the water displacement method. All reactions were carried out at room temperature. Before testing the

catalytic performance of the catalysts, they were reduced in 0.075 M NaBH<sub>4</sub>-solution.

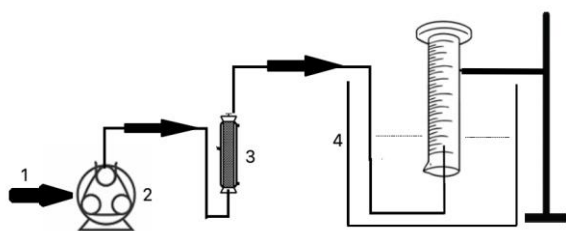


**Figure 1.** The scheme of the catalytic performance system (1: inlet solution, 2: peristaltic pump, 3: fix-bed reactor, 4: gas collection (water displacement method))

### 3. Results and Discussions

#### 3.1. Characterization of catalysts

Pristine alumina pellets possess a high surface area of 212.48 m<sup>2</sup>·g<sup>-1</sup>. In Table 1, the BET surface areas of Ni/Al<sub>2</sub>O<sub>3</sub>, NiCo/Al<sub>2</sub>O<sub>3</sub>, and Ru-NiCo/Al<sub>2</sub>O<sub>3</sub> catalysts were listed, and a decrease in the specific surface area has been noticed. These results revealed that the alumina pellets have been successfully coated with the relevant metal oxide structure. In addition, the NiCo/Al<sub>2</sub>O<sub>3</sub> catalyst has

the highest, and because of the additional coating procedure, the catalyst Ru-NiCo/Al<sub>2</sub>O<sub>3</sub> possess the lowest specific surface area, as expected. ICP-MS analyses have been conducted to determine the metal contents in each catalyst. NiCo/Al<sub>2</sub>O<sub>3</sub> and Ru-NiCo/Al<sub>2</sub>O<sub>3</sub> catalysts have similar Co and Ni content, however, in Ru-NiCo/Al<sub>2</sub>O<sub>3</sub> catalyst, the presence of Ru has been detected which shows that the coating with RuO<sub>2</sub> has been accomplished. The crystal phases of all catalysts were determined by XRD analyses, and XRD patterns are shown in Figure 2. The diffraction pattern of pristine alumina displays significant peaks at 2θ of 37.12°, 39.49°, 45.06°, and 67.52°. The Ni/Al<sub>2</sub>O<sub>3</sub> catalyst possesses peaks at 2θ of 37.11°, 45.14°, 59.81°, and 65.75°, which are assigned to the crystal phase of NiAl<sub>2</sub>O<sub>4</sub>. Furthermore, the presence of the NiAl<sub>2</sub>O<sub>4</sub> phase indicates that the Ni<sup>2+</sup> cations were successfully incorporated into the alumina structure. The XRD pattern of the NiCo/Al<sub>2</sub>O<sub>3</sub> catalyst shows the characteristic peaks for the Co<sub>2</sub>NiO<sub>4</sub> crystal phase at 2θ of 37.32°, 60.18° and 66.16°. Herein, these results confirm the deposition of Co<sub>2</sub>NiO<sub>4</sub> on the alumina. The Ru-NiCo/Al<sub>2</sub>O<sub>3</sub> catalyst differs from the NiCo/Al<sub>2</sub>O<sub>3</sub> through RuO coating, and the presence of RuO has been proved at 2θ of 28.30° and 54.45°.

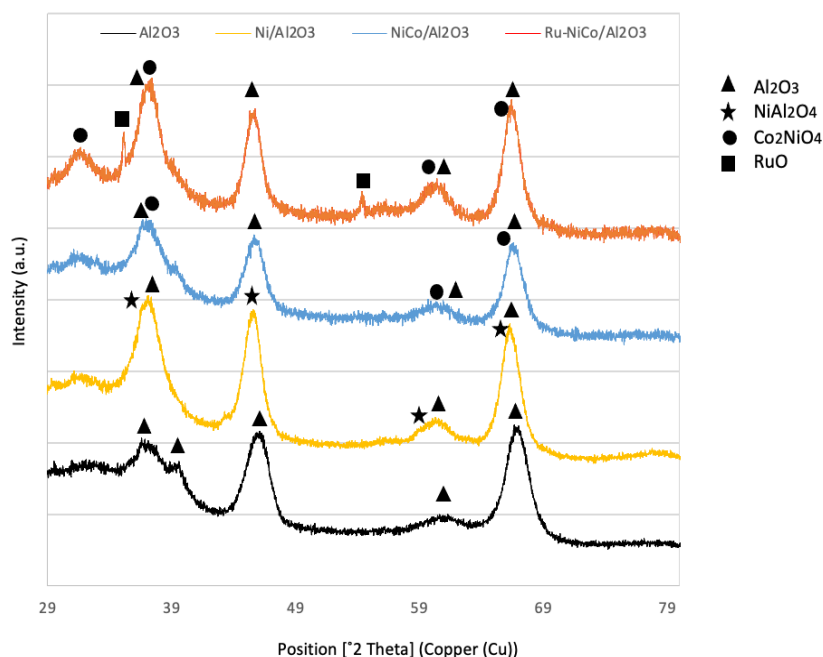


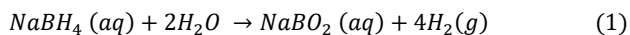
**Figure 2.** XRD patterns of all synthesized catalysts.

**Table 1.** Synthesized catalysts with their crystal phases by XRD, metal contents by ICP-MS and specific surface areas by BET

| Code for catalysts                     | Crystal phases by XRD<br>(Reference Code)  | Metal contents by ICP-MS |             |             |             | BET (m <sup>2</sup> ·g <sup>-1</sup> ) |
|--|--|--------------------------|-------------|-------------|-------------|--|
|  |  | Ru (wt %)                | Co (wt %)   | Ni (wt %)   | Al (wt %)   |  |
| Ni/Al <sub>2</sub> O <sub>3</sub>      | NiAl <sub>2</sub> O <sub>4</sub> (01-078-6954)<br>Al <sub>2</sub> O <sub>3</sub> (00-056-1186)                                   | -                        | -           | 8.20 ± 0.16 | 31.54 ± 2.1 | 165.44                                 |
| NiCo/Al <sub>2</sub> O <sub>3</sub>    | Co <sub>2</sub> NiO <sub>4</sub> (04-018-4105)<br>Al <sub>2</sub> O <sub>3</sub> (00-056-1186)                                   | -                        | 4.16 ± 0.22 | 2.86 ± 0.05 | 32.55 ± 2.2 | 165.84                                 |
| Ru-NiCo/Al <sub>2</sub> O <sub>3</sub> | RuO <sub>2</sub> (00-040-1290)<br>Co <sub>2</sub> NiO <sub>4</sub> (04-018-4105)<br>Al <sub>2</sub> O <sub>3</sub> (00-056-1186) | 0.02 ± 0.0024            | 3.96 ± 0.21 | 2.89 ± 0.06 | 31.32 ± 2.1 | 154.40                                 |

### 3.2. Catalytic hydrolysis of NaBH<sub>4</sub>

The hydrogen generation through NaBH<sub>4</sub> hydrolysis takes place through the following reaction (Equation (1)) (Liu and Li 2009). In this process, 0.5 M NaBH<sub>4</sub> solution was fed to the reactor continuously, and hydrogen generation was measured by the water displacement method.



Firstly, the catalytic performance of the pristine alumina was tested to understand whether the alumina pellets have a catalytic effect on the hydrolysis reaction. As a result, in the presence of pristine alumina, no hydrogen generation was observed. The three synthesized different catalysts have been tested in this continuous flow reactor at the same reaction parameters. Among these catalysts, the Ni/Al<sub>2</sub>O<sub>3</sub> sample exhibited poor hydrogen generation which shows that the monometallic Ni coating did not improve the catalytic performance of alumina. Additionally, regarding the XRD results, it can be concluded that NiAl<sub>2</sub>O<sub>4</sub> species are not active phases to dissociate NaBH<sub>4</sub>.

On the other hand, the NiCo/Al<sub>2</sub>O<sub>3</sub> catalyst showed a promising catalytic activity as demonstrated in Figure 3a and 3b. In the presence of this type of catalyst, the initial hydrogen generation rate was slow, but it increased continuously. The behavior of this catalyst can be attributed to the presence of inactivated catalyst species that are activated after self-reduction with the generation of H<sub>2</sub>. After a 2h reaction, the H<sub>2</sub> generation rate rises to

0.0014 mmol·s<sup>-1</sup>·g<sup>-1</sup>. As a result, it can be said that the Co<sub>2</sub>NiO<sub>4</sub> crystal phase acts as an active species for the dissociation of NaBH<sub>4</sub> molecules.

The addition of RuO into the catalyst structure has a significant improvement on the performance of NiCo/Al<sub>2</sub>O<sub>3</sub> catalyst as seen in Figure 3c and 3d. In the presence of the Ru-NiCo/Al<sub>2</sub>O<sub>3</sub> catalyst, the hydrolysis reaction starts with a reaction rate of 0.031 mmol·s<sup>-1</sup>·g<sup>-1</sup>, but the reaction rate decreases rapidly and the hydrogen generation rate sinks to 0.005 mmol·s<sup>-1</sup>·g<sup>-1</sup>. The behavior of the catalyst can be assigned to the deactivation of Ru species through the accumulation of Na-based compounds on the catalyst surface (Arzac et al. 2012).

Table 2 gives an insight into the performances of various catalysts from the literature comparable with results from the present study. Here, it can be concluded that the alumina-supported catalysts in powder form exhibited higher H<sub>2</sub> generation due to its higher amount of active metal sites on the catalyst surface (Xu et al. 2007). However, in the presence of a catalyst supported on ceramic foam (Balkanlı and Figen 2019) or cylindrical pellets (Su et al. 2012), H<sub>2</sub> generation is significantly lower than in the presence of the powder catalyst. In this study, despite the lower concentration of NaBH<sub>4</sub> solution and lower amount of noble metal (Ru) in the catalyst structure, a maximum H<sub>2</sub> generation rate of 50.4 ml·min<sup>-1</sup>·g<sup>-1</sup> was achieved. In addition, it is expected that with an increase in the concentration of NaBH<sub>4</sub> solution achievement of higher H<sub>2</sub> generation compared to those stated in the literature is possible.

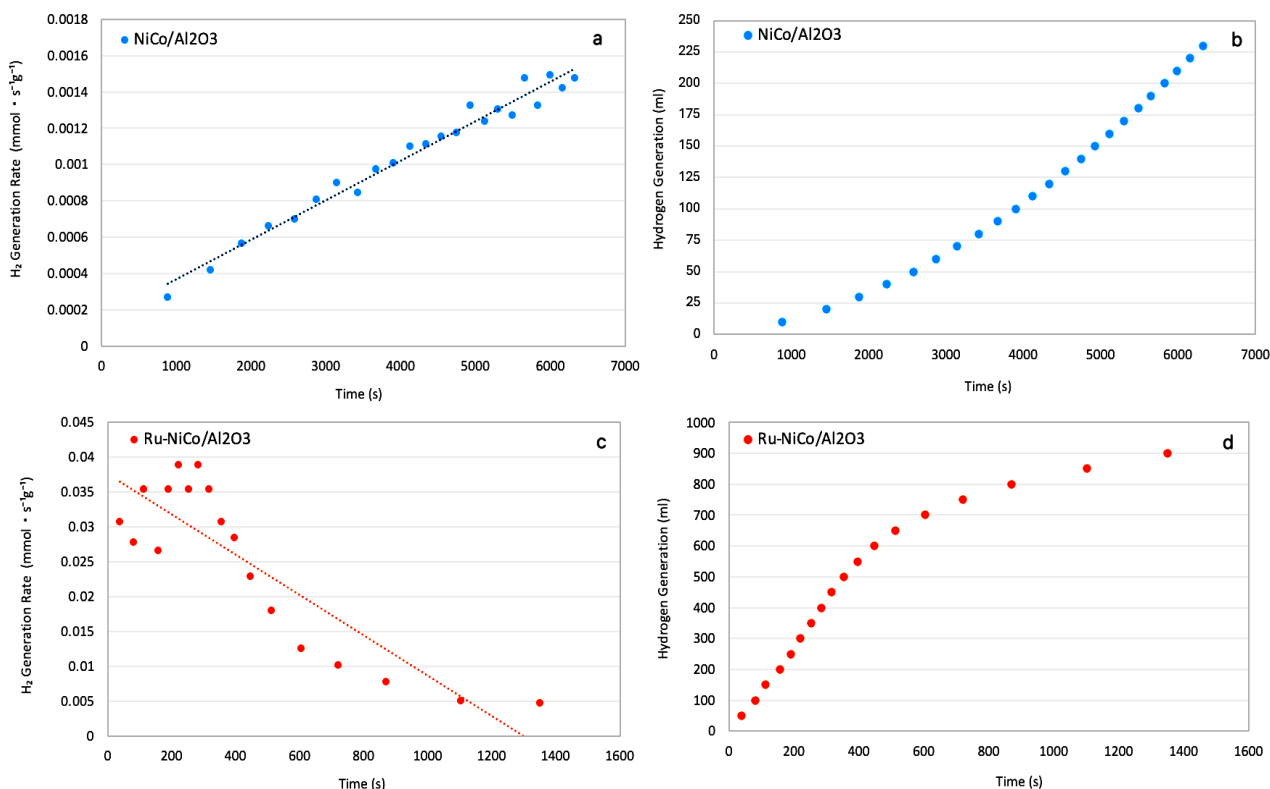


**Figure 3.** Hydrogen generation from NaBH<sub>4</sub> in the presence of NiCo/Al<sub>2</sub>O<sub>3</sub> and Ru-NiCo/Al<sub>2</sub>O<sub>3</sub> catalysts at 25 °C.

**Table 2.** Comparison of the results from the present study with those in the literature

| Catalyst composition                                  | Support form | T (°C) | NaBH <sub>4</sub> solution           | Max. H <sub>2</sub> generation             | Ref.                    |
|---|--------------|--------|--------------------------------------|--|-------------------------|
| 0.05 wt% Pd-4.7 wt% LiCo/SiC-based ceramic foam       | Ceramic foam | 25     | cNaBH <sub>4</sub> : cNaOH=1:1       | 4.76 ml·min <sup>-1</sup>                  | Balkanli and Figen 2019 |
| 5 wt% Ru/Al <sub>2</sub> O <sub>3</sub>               | Pellet       | 25     | 10 wt% NaBH <sub>4</sub> -1 wt% NaOH | 65.5 ml·min <sup>-1</sup> ·g <sup>-1</sup> | Su et al. 2012          |
| 2 wt% Pt/Al <sub>2</sub> O <sub>3</sub>               | Powder       | 30     | 10 wt% NaBH <sub>4</sub> -5 wt% NaOH | 8510 ml·min <sup>-1</sup> ·g <sup>-1</sup> | Xu et al. 2007          |
| 7 wt% NiCo/Al <sub>2</sub> O <sub>3</sub>             | Pellet       | 25     | 2 wt% NaBH <sub>4</sub> -2 wt% NaOH  | 2.2 ml·min <sup>-1</sup> ·g <sup>-1</sup>  | Present study           |
| 0.02 wt% Ru-7 wt% NiCo/Al <sub>2</sub> O <sub>3</sub> | Pellet       | 25     | 2 wt% NaBH <sub>4</sub> -2 wt% NaOH  | 50.4 ml·min <sup>-1</sup> ·g <sup>-1</sup> | Present study           |

#### 4. Conclusions

In summary, the high-surface area alumina pellets have been proposed as an effective support material for the catalysts in the hydrolysis reaction of NaBH<sub>4</sub>. Alumina samples loaded with metal oxides were successfully prepared via the wash coating method. Results revealed that Co<sub>2</sub>NiO<sub>4</sub> species form active centers for the dissociation of NaBH<sub>4</sub> molecules. Consequently, the Ru-NiCo/Al<sub>2</sub>O<sub>3</sub> catalyst exhibited the highest initial hydrogen generation rate, however, the NiCo/Al<sub>2</sub>O<sub>3</sub> catalyst can be proposed as a promising alternative due to its increasing catalytic performance during the reaction.

#### Declaration of Ethical Standards

The authors declare that they comply with all ethical standards.

#### Declaration of Competing Interest

The authors have no conflicts of interest to declare regarding the content of this article.

#### Data Availability

All data generated or analyzed during this study are included in this published article.

#### 5. References

- Arzac, G. M., Hufschmidt, D., Jimenes De Haro, M. C., Fernandez, A., Sarmiento, B., Jimenez, M. A., Jimenez, M. M., 2012. Deactivation, reactivation and memory effect on Co-B catalyst for sodium borohydride hydrolysis operating in high conversion conditions. *International Journal of Hydrogen*, **37**, 14373-14381. <https://doi.org/10.1016/j.ijhydene.2012.06.117>
- Balkanli, E. and Figen, H. E., 2019. Sodium borohydride hydrolysis by using ceramic foam supported bimetallic and trimetallic catalysts. *International Journal of Hydrogen*, **44**, 9959-9969. <https://doi.org/10.1016/j.ijhydene.2018.12.010>
- Baykara S., 2018. Hydrogen: A brief overview on its sources, production and environmental impact. *International Journal of Hydrogen*, **43**, 10605-10614. <https://doi.org/10.1016/j.ijhydene.2018.02.022>
- Baykara, Z. S., Figen, H. E., Karaismailoğlu, M., (2022). Environmental issues with hydrogen production. *Comprehensive Renewable Energy, Second Edition*, Amsterdam: Elsevier Science, Oxford/Amsterdam, 107-126. <https://doi.org/10.1016/B978-0-12-819727-1.00025-X>
- Bozkurt, G., Özer, A., Yurtcan, A. B., 2019. Development of effective catalysts for hydrogen generation from sodium borohydride: Ru, Pt, Pd nanoparticles supported on Co<sub>3</sub>O<sub>4</sub>. *Energy*, **180**, 702-713. <https://doi.org/10.1016/j.energy.2019.04.196>
- Fernandes, R, Patel, N., Miotello, A., 2009. Hydrogen generation by hydrolysis of alkaline NaBH<sub>4</sub> solution with Cr-promoted Co-B amorphous catalyst. *Applied Catalysis B: Environmental*, **92**, 68-74. <https://doi.org/10.1016/j.apcatb.2009.07.019>
- Filiz, B. C. and Figen, A. K., 2019. Hydrogen production from sodium borohydride originated compounds: Fabrication of electrospun nano-crystalline Co<sub>3</sub>O<sub>4</sub> catalyst and its activity. *International Journal of Hydrogen*, **20**, 9883-9895. <https://doi.org/10.1016/j.ijhydene.2019.02.111>
- Laversenne, L., Goutaudier, C., Chiriach, R., Sigala, C., Bonnetot, B., 2008. Hydrogen storage in borohydrides Comparison of hydrolysis conditions of LiBH<sub>4</sub>, NaBH<sub>4</sub> and KBH<sub>4</sub>. *Journal of Thermal Analysis and Calorimetry*, **94**, 785-790. <https://doi.org/10.1007/s10973-008-9073-4>
- Liu, B. H. and Li, Z. P., 2009. A review: hydrogen generation from borohydride hydrolysis reaction. *Journal of Power Sources*, **187**, 527-534. <https://doi.org/10.1016/j.jpowsour.2008.11.032>
- Luo, Y., Wang, Q., Li, J., Xu, F., Sun, L., Zou, Y., Chu, H., Li, B., Zhang, K., 2020. Enhanced hydrogen storage/sensing of metal hydrides by nano-modification. *Materials Today Nano*, **9**, 10071-10100. <https://doi.org/10.1016/j.mtnano.2019.100071>
- Patel, N. and Miotello, A., 2015. Progress in Co-B related catalyst for hydrogen production by hydrolysis of

- boron-hydrides: A review and the perspectives to substitute noble metals. *International Journal of Hydrogen*, **40**, 1429-1464.  
<https://doi.org/10.1016/j.ijhydene.2014.11.052>
- Özkar, S. and Zahmakiran M., 2005. Hydrogen generation from hydrolysis of sodium borohydride using Ru(0) nanoclusters as catalyst. *Journal of Alloys and Compounds*, **404-406**, 728-731.  
<https://doi.org/10.1016/j.jallcom.2004.10.084>
- Schlesinger, H. I., Brown, H. C., Finholt, A. E., Gilbreath, J. R., Hoekstra, H. R., & Hyde, E. K. (1953). Sodium borohydride, its hydrolysis and its use as a reducing agent and in the generation of hydrogen<sup>1</sup>. *Journal of the American Chemical Society*, **75**, 215-219.  
<https://doi.org/10.1021/ja01097a057>
- Schneemann, A., White, J. L., Kang, S., Jeong, S., Wan, L. F., Cho, E. S., Heo, T. W., Prendergast, D., Urban, J. J., Wood, B. C., Allendorf, M. D., Stavila, V., 2018. Nanostructured metal hydrides for hydrogen storage. *Chemical Reviews*, **118**, 10775-10839.  
<https://doi.org/10.1021/acs.chemrev.8b00313>
- Solovev, M. V., Chashchikhin, O. V., Dorovatovski, P. V., Khrustalev, V. N., Zyubin, A. S., Zyubina, T. S., Kravchenko, O. V., Zaytsev, A. A., Dobrovosky, Y. A., 2018. Hydrolysis of Mg(BH<sub>4</sub>)<sub>2</sub> and its coordination compounds as a way to obtain hydrogen. *Journal of Power Sources*, **377**, 93-102.  
<https://doi.org/10.1016/j.jpowsour.2017.11.090>
- Su, C-C., Lu, M-C., Wang, S-L., Huang, Y-H. (2012). Ruthenium immobilized on Al<sub>2</sub>O<sub>3</sub> pellets as a catalyst for hydrogen generation from hydrolysis and methanolysis of sodium borohydride. *RSC Advances*, **2**, 2073-2079.  
<https://doi.org/10.1039/c2ra01233b>
- Uzundurukan, A. and Devrim., Y., 2019. Hydrogen generation from sodium borohydride hydrolysis by multi-walled carbon nanotube supported platinum catalyst: A kinetic study. *International Journal of Hydrogen*, **44**, 17586-17594.  
<https://doi.org/10.1016/j.ijhydene.2019.04.188>
- Xu, D., Zhang, H. Ye, W. (2007). Hydrogen generation from hydrolysis of alkaline sodium borohydride solution using Pt/C catalyst. *Catalysis Communications*, **8**, 1767-1771.  
<https://doi.org/10.1016/j.catcom.2007.02.028>
- Xu, F., Ren, J., Ma, J., Wang, Y., Zhang, K., Cao, Z., Sun, Q., Wu, S., Li, G., Bai, S., 2024. A review of hydrogen production kinetics from the hydrolysis of NaBH<sub>4</sub> solution catalyzed by Co-based catalysts. *International Journal of Hydrogen*, **50**, 827-844.  
<https://doi.org/10.1016/j.ijhydene.2023.08.142>
- Wang, Y., Hu, Z., Chen, W., Wu, S., Li, G., Chou, S., 2021. Non-noble metal-based catalysts applied to hydrogen evolution from hydrolysis of boron hydrides. *Small*, **2**, 2000135-2000161.  
<https://doi.org/10.1002/ssstr.202000135>
- Yang, C. C., Chen, M. S., Chen, Y. W., 2011. Hydrogen generation by hydrolysis of sodium borohydride on CoB/SiO<sub>2</sub> catalyst. *International Journal of Hydrogen*, **36**, 1418-1423.  
<https://doi.org/10.1016/j.ijhydene.2010.11.006>
- Zhang H., Zhang, L., Rodriguez-Perez, I. A., Miao, W., Chen, K., Wang, W., Li, Y., Han, S., 2021. Carbon nanospheres supported bimetallic Pt-Co as an efficient catalyst for NaBH<sub>4</sub> hydrolysis. *Applied Surface Science*, **540**, 148296-148304.  
<https://doi.org/10.1016/j.apsusc.2020.148296>
- Zhu, Y., Li, J., Yang, L., Huang, Z., Yang X-S., Zhou, Q., Tang, R., Shen, S. and Ouyang, L., 2023. Closed loops for hydrogen storage: Hydrolysis and regeneration of metal borohydrides. *Journal of Power Sources*, **563**, 232833-232847.  
<https://doi.org/10.1016/j.jpowsour.2023.232833>